

Kinetics of styrene emulsion polymerization in the presence of montmorillonite

Chorng-Shyan Chern^{a,*}, Jiang-Jen Lin^b, Yan-Liang Lin^a, Shu-Zhen Lai^a

^a Department of Chemical Engineering, National Taiwan University of Science and Technology, Taipei 106, Taiwan, ROC

^b Institute of Polymer Science and Engineering, National Taiwan University, Taipei 106, Taiwan, ROC

Received 5 September 2005; received in revised form 31 October 2005; accepted 2 November 2005

Available online 22 December 2005

Abstract

The effect of the pristine sodium montmorillonite (Na^+ -MMT) on the styrene emulsion polymerizations with different concentrations of SDS ([SDS]) was investigated. At constant [SDS], the polymerization rate is faster for the run with 1 wt.% Na^+ -MMT compared to the counterpart without Na^+ -MMT. Micelle nucleation predominates in the polymerizations with $[\text{SDS}] \geq 13$ mM. On the other hand, the contribution of the polymerization associated with the Na^+ -MMT platelets increases significantly when [SDS] decreases from 13 to 9 mM. At $[\text{SDS}]$ (e.g., 2 mM) < CMC, homogeneous nucleation controls the particle formation process and polymerization kinetics. Moreover, the contribution of the Na^+ -MMT platelets that act as extra reaction loci to the polymerization kinetics is even comparable to the run in the absence of Na^+ -MMT. The resultant polymer particle size, polymer molecular weight and zeta potential were characterized and a preliminary model was developed to qualitatively study the differences between the polymerizations in the presence and absence of 1 wt.% Na^+ -MMT.

© 2005 Elsevier Ltd. All rights reserved.

Keywords: Styrene emulsion polymerization; Montmorillonite; Kinetics

1. Introduction

Emulsion polymerization involves the propagation reaction of free radicals with monomer within the monomer-swollen polymer particles dispersed in the continuous aqueous phase. The discrete hydrophobic particles are stabilized by surfactant such as the anionic sodium dodecyl sulfate (SDS). When the level of surfactant is greater than its critical micelle concentration (CMC), the polymeriza-

tion kinetics can be adequately predicted by the Smith–Ewart theory [1–6]. Particle nuclei are generated via the capture of radicals by micelles, termed the micelle nucleation. On the other hand, the polymerization with the surfactant concentration below its CMC is characterized by homogeneous nucleation [7–11]. The water-borne radical becomes insoluble and forms a particle nucleus when a critical chain length is achieved. This is followed by the formation of stable primary particles via the limited flocculation of unstable particle nuclei and adsorption of surfactant on their particle surfaces. The rate of polymerization (R_p) is linearly proportional to the number of particles nucleated per liter water

* Corresponding author. Tel.: +886 2 27376649; fax: +886 2 27376644.

E-mail address: cschern@mail.ntust.edu.tw (C.-S. Chern).

(N_p) and average number of radicals per particle (n): $R_p = k_p[M]_p(nN_p/N_A)$, where k_p is the propagation rate constant, $[M]_p$ is the concentration of monomer in the particles and N_A is the Avogadro number.

Inorganic materials such as the cost effective sodium montmorillonite (Na^+ -MMT) are generally added into latex products to improve their physical properties. Recently, emulsion polymerizations of various monomers in the presence of Na^+ -MMT were investigated and the resultant composite materials characterized [12–16]. Kim et al. [14] prepared intercalated hydrophobic polystyrene (PS)/ Na^+ -MMT composite particles via emulsion polymerization without resort to the ionic exchanging process. It was shown that emulsion polymerization is an effective process for synthesizing the intercalated PS/ Na^+ -MMT particles. This is due to the fact that the interlayers of Na^+ -MMT are filled with Na^+ ions and, therefore, the hydrophilic Na^+ -MMT platelets are highly swollen in water. This will then promote the penetration of the water-borne oligomeric radicals into the multiple-layered Na^+ -MMT. However, to the best of our knowledge, the literature dealing with the kinetics of the styrene (ST) emulsion polymerization in the presence of Na^+ -MMT is nil. The goal of this work was therefore to gain a better understanding of the role of Na^+ -MMT in the ST emulsion polymerization initiated by sodium persulfate (SPS) and stabilized by SDS.

2. Experimental

2.1. Materials

ST (Taiwan Styrene), Na^+ -MMT (Kunimine Ind., a smectite silicate clay with a cationic exchange capacity of 1.15 meq g^{-1}), SDS (J.T. Baker, 99%), SPS (Riedel-de Haen), sodium bicarbonate (Janssen Chimica), hydroquinone (Nacalia Tesque), sodium chloride (J.T. Baker), methanol (Acros), a series of PS standards for GPC calibration (Shodex), tetrahydrofuran (THF; Merk), nitrogen (Ching-Feng-Harng), and deionized water (Barnsted Nanopure Ultrapure Water System, specific conductance $<0.057 \mu\text{S cm}^{-1}$) were used in this work. ST was distilled at 40°C under reduced pressure. All other chemicals were used as received.

2.2. Experimental methods

The CMC of the aqueous solution of SDS in the presence or absence of Na^+ -MMT was determined

by the electric conductance technique (Orion, Model 115) [17–19]. The concentrations of NaHCO_3 (buffer) and Na^+ -MMT were set at 2.59 mM and 1 wt.%, respectively, in the conductivity measurements. For the Na^+ -MMT suspension, the sample was first subject to ultrasonication (Ultrasonics, Sonicator W385) for 15 min and it was then stirred using a 45° -pitched 4-bladed agitator at 200 rpm and 30°C for 20 min. Note that the suspension at the time of the conductivity measurement was kinetically stable. Thus, 1 min before the start of measurement, the agitation was stopped and the average of three measurements at 0.5, 1 and 1.5 min was reported as the conductivity (κ). The above procedure was repeated for different concentrations of SDS [SDS]. The CMC was then determined from the break of the slope on the κ vs. [SDS] curve.

To assure the uniformity and reproducibility of the suspensions in emulsion polymerization experiments, the pristine clay was added slowly to the mixture containing H_2O , NaHCO_3 and SDS with the aid of a mechanical homogenizer (Janke & Kunkel, Ultra-Turrax T25) operated at 8000, 9500 and then 13500 rpm (10 min for each homogenization step). This was followed by charging the Na^+ -MMT suspension and ST in sequence to a 750-ml reactor equipped with a 45° -pitched 4-bladed agitator, a thermometer, and a reflux condenser. The reaction mixture was purged with N_2 to remove the dissolved O_2 for 30 min before the start of polymerization initiated by 2.59 mM SPS. The temperature was controlled within $70 \pm 0.5^\circ\text{C}$ and the agitation speed was kept constant at 250 rpm throughout the reaction. The total solid content of the latex product is about 16% for complete monomer conversion. The product was filtered through 40-mesh (0.42 mm) and 200-mesh (0.074 mm) screens in series to collect filterable solids. Scraps adhering to the agitator, thermometer, and reactor wall were also collected. The levels of filterable solids and scraps obtained from all the polymerizations were negligible. These results showed that satisfactory colloidal stability during the reaction was achieved for the recipes and polymerization conditions used in this work. The total solid content and conversion of ST(X) were determined gravimetrically. The weight-average particle diameter (d_w), volume-average particle diameter (d_v) and polydispersity index of the particle size distribution ($\text{PDI} = d_w/d_n$) were measured by transmission electron microscopy (TEM, JEOL TEM-1200 EXII). The parameter d_n is the num-

ber-average particle diameter. At least 300 spherical particles per sample were counted in the particle size measurement. Based on the d_v data, the number of particles per liter water produced at the end of polymerization without Na^+ -MMT (N_p) was calculated.

The zeta potential of colloidal particles (ζ) was measured with the Malvern Zetamaster. The dilution solution for the sample (total solid content = 0.01%) was 0.01 M NaCl. The reported ζ data represent an average of at least 10 measurements. Latex particles were precipitated by an excess of methanol, followed by thorough washes with methanol and water to remove residual SDS and other impurities. The dried PS/ Na^+ -MMT composite was dissolved in THF ($\approx 2 \times 10^{-3} \text{ g cm}^{-3}$). The weight-average polymer molecular weight (M_w) was determined by gel permeation chromatography (GPC; Waters 515/2410/Styragel HR2, HR4, and HR6) calibrated by a series of PS standards (Shodex). The sample was filtered by a $0.45 \mu\text{m}$ membrane immediately before the GPC measurement. X-ray powder diffraction (XRD) analysis was performed by a diffractometer (MAC Science MXP18) with a Cu target ($\lambda = 1.54 \times 10^{-10} \text{ m}$) at a generator voltage of 30 kV, a generator current of 25 mA, and a scanning rate of 4° min^{-1} .

3. Results and discussion

Representative κ vs. [SDS] data are shown in Fig. 1. The CMC of the aqueous solution of SDS and 2.59 mM NaHCO_3 is 8.3 mM, which is very close to those of the aqueous SDS solutions in the absence of NaHCO_3 [20,21]. However, incorporation of 1 wt.% Na^+ -MMT reduces the CMC to 6.4 mM. This implies that the Na^+ -MMT platelet surfaces are relatively hydrophilic and, thus, not effective for the adsorption of SDS. Another factor is the much higher ionic strength of the Na^+ -MMT-containing SDS solution compared to the native SDS solution, as shown by the magnitudes of the κ data in Fig. 1. SDS molecules subject to the hostile environment with a very high electrolyte concentration show a stronger tendency to aggregate with one another to form micelles. This will then result in the decreased CMC. The CMC values are expected to have an influence on the concentration of micelles available for particle nucleation (i.e., polymerization kinetics).

Representative X vs. time (t) curves for the ST emulsion polymerizations in the presence of

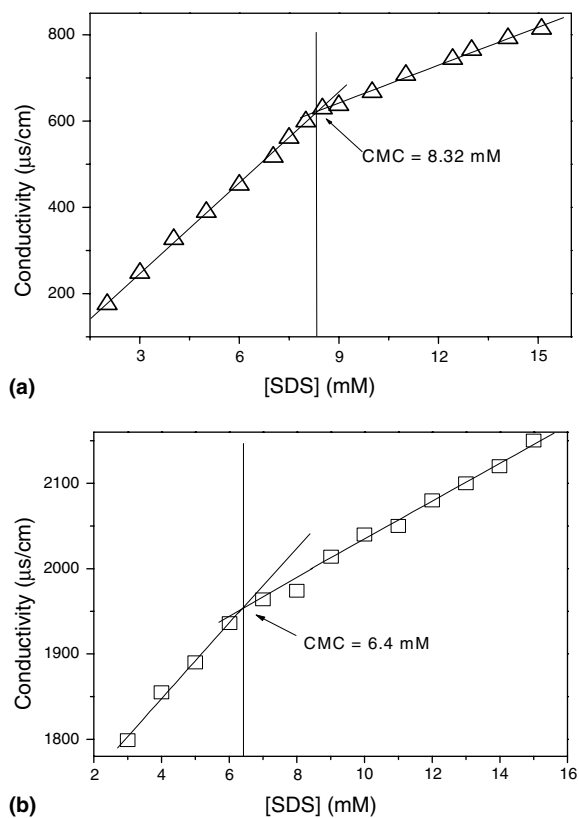


Fig. 1. Specific conductivity of SDS as a function of the bulk SDS concentration. (a) SDS; (b) SDS + 1 wt.% Na^+ -MMT.

1 wt.% Na^+ -MMT and 2–19 mM SDS are shown in Fig. 2. For comparison, in the absence of Na^+ -MMT, the ST emulsion polymerization with $[\text{SDS}] = 2 \text{ mM}$ is also included in Fig. 2b. The experiment was carried out twice and the reproducibility was quite satisfactory. The rate of polymerization ($R_p = [\text{M}]_0 dX/dt$) data as a function of $[\text{SDS}]$ are shown in Fig. 3, where $[\text{M}]_0$ is the initial monomer concentration based on total water (1.7 M) and the value of dX/dt is obtained from the least-squares-best-fitted slope of the linear portion of the X vs. t curve. The range of the kinetic data used to determine the value of dX/dt was dependent on $[\text{SDS}]$ due to the different particle nucleation periods and gel effects associated with different particle sizes at high conversion. The correlations based on the kinetic data are $R_p \sim [\text{SDS}]^{0.79}$ [coefficient of determination (r^2) = 0.9595] and $R_p \sim [\text{SDS}]^{0.85}$ ($r^2 = 0.9667$) for the runs with and without 1 wt.% Na^+ -MMT, respectively. At constant $[\text{SDS}]$, R_p is faster for the run containing Na^+ -MMT compared to the counterpart without Na^+ -MMT. The enhanced R_p for the polymerizations

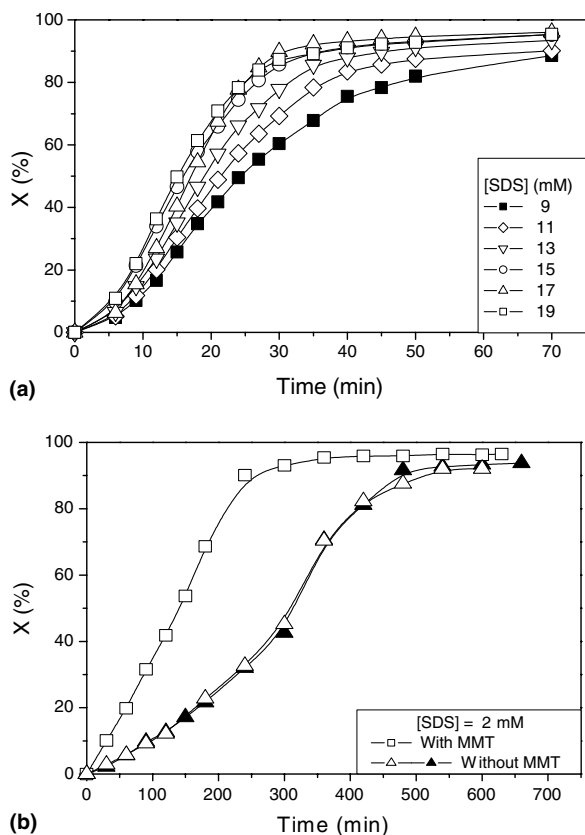


Fig. 2. Conversion as a function of time for the ST emulsion polymerizations in the presence of 1 wt.% Na^+ -MMT and various bulk SDS concentrations. (a) $[\text{SDS}]$ (mM) = (\square) 19, (Δ) 17, (\circ) 15, (∇) 13, (\diamond) 11, (\blacksquare) 9; (b) $[\text{SDS}] = 2$ mM and Na^+ -MMT (wt.%) = (\square) 1, (Δ) 0.

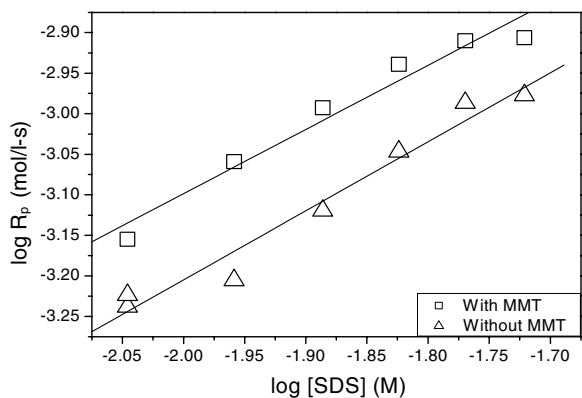


Fig. 3. Rate of polymerization as a function of the bulk SDS concentration. Na^+ -MMT (wt.%) = (\square) 1, (Δ) 0.

containing Na^+ -MMT might be due to the larger number of micelles (N_m) available for particle nucleation provided that $[\text{SDS}]$ is above its CMC. Chang

et al. [19] showed that the fraction of SDS adsorbed on the ST droplet surfaces is insignificant compared to that associated with the monomer-swollen micelles. The data of the aggregation number of SDS molecules per micelle ($n_{\text{agg,m}}$) obtained from the literature [22] follow the following least-squares-best-fitted relationship:

$$n_{\text{agg,m}} = 83.201[\text{NaCl}] + 94.295 \quad (r^2 = 0.7705) \quad (1)$$

where $[\text{NaCl}]$ is the sodium chloride concentration. Although the data are somewhat scattered, about 33% increase in $n_{\text{agg,m}}$ is obtained when $[\text{NaCl}]$ increases from 0.02 to 0.4 M (i.e., a twentyfold increase in $[\text{NaCl}]$). Fig. 1 shows that, for example, the conductivity (or ionic strength) of the aqueous SDS solution in the presence of 1 wt.% Na^+ -MMT at CMC is only about three times as large as that of the aqueous SDS solution at CMC. Thus, the values of $n_{\text{agg,m}}$ should not change much for the polymerization recipes investigated in this study. To simplify the following estimation, the effect of ionic strength on $n_{\text{agg,m}}$ is neglected at this moment. Further assuming that the fraction of SDS adsorbed on both the monomer droplet surfaces and 1 wt.% Na^+ -MMT platelet surfaces is negligible and taking the polymerization with $[\text{SDS}] = 13$ mM as an example, the maximal increase of N_m due to the presence of 1 wt.% Na^+ -MMT is $[(13 - 6.4)/(13 - 8.3) - 1] \times 100\% = 40\%$ (Table 1). The corresponding increase of R_p due to the presence of 1 wt.% Na^+ -MMT is $[(9.97 \times 10^{-4} - 7.60 \times 10^{-4})/7.60 \times 10^{-4}] \times 100\% = 31\%$. Table 1 shows that micelle nucleation plays an important role in the polymerizations with $[\text{SDS}] \geq 13$ mM. On the other hand, other parameters must come into play for the polymerizations with $[\text{SDS}] < 13$ mM, especially for the run with $[\text{SDS}] = 2$ mM.

R_p is linearly proportional to the product of the number of reaction loci (N_p) and the average number of radicals per particle (n). N_p is primarily determined by the concentration of micelles available for particle nucleation for the polymerizations with $[\text{SDS}] > \text{CMC}$. In the absence of micelles, N_p is controlled by the amount of SDS available for stabilizing the particles generated by homogeneous nucleation. Fig. 4 shows (a) a representative TEM photograph for the Na^+ -MMT-containing polymerization with $[\text{SDS}] = 13$ mM, (b) the final latex particle diameter (d_v) and (c) the particle size distribution (PDI) as a function of $[\text{SDS}]$. It is shown that d_v decreases with increasing $[\text{SDS}]$ for both the polymerizations with and without Na^+ -MMT. At

Table 1

Theoretical calculation of the maximal increase of N_m and the corresponding increase of R_p due to the presence of 1 wt.% Na⁺-MMT for ST emulsion polymerization

[SDS] (mM)	2	9	11	13	15	17	19
$[(\text{[SDS]} - \text{CMC})/(\text{[SDS]} - \text{CMC}_0) - 1] \times 100\%^a$	–	271	70	40	28	22	18
$(R_p - R_{p,0})/R_{p,0} \times 100\%^b$	113	17	40	31	28	14	16

^a CMC and CMC₀ represent the critical micelle concentration in the presence of and in the absence of Na⁺-MMT, respectively.

^b R_p and $R_{p,0}$ represent the polymerization rate in the presence of and in the absence of Na⁺-MMT, respectively.

constant [SDS], the run with Na⁺-MMT has a smaller particle size compared to the counterpart without Na⁺-MMT. This is attributed to the larger population of particles originating from micelle nucleation as a result of the lowered CMC along with the smaller fraction of polymer produced in these particles. PDI increases slightly with increasing [SDS] for the polymerizations with Na⁺-MMT, but it remains relatively constant for the polymerizations without Na⁺-MMT. For constant polymer weight, N_p is inversely proportional to d_v . Without the knowledge of the fraction of polymer produced in the particles originating from micelle nucleation, we were unable to obtain the N_p data from TEM measurements because the propagation reaction of radicals with monomer in the Na⁺-MMT platelets cannot be ignored [16]. Independent experiments are required to differentiate the polymer chains produced in the particles originating from micelle nucleation and those produced in the Na⁺-MMT platelets. It is postulated that the reaction systems with [SDS] \geq 13 mM are so abundant in micelles that the polymerization kinetics is predominated by micelle nucleation. Under the circumstances, the contribution of Na⁺-MMT platelets to the polymerization kinetics is not important. At [SDS] < 13 mM, on the other hand, the contribution of the polymerization associated with Na⁺-MMT platelets increases significantly when [SDS] decreases from 13 to 9 mM. At [SDS] = 2 mM, micelles do not exist in the polymerization system. It is therefore the homogeneous nucleation that controls the polymerization kinetics. The contribution of Na⁺-MMT platelets to the polymerization kinetics is now even comparable to the run without Na⁺-MMT ($R_p = 4.80 \times 10^{-5} \text{ mol dm}^{-3} \text{ s}^{-1}$) provided that, as a first approximation, the contribution of Na⁺-MMT platelets can be estimated to be the difference between the polymerization rate in the presence of Na⁺-MMT ($R_p = 1.02 \times 10^{-4} \text{ mol dm}^{-3} \text{ s}^{-1}$) and the polymerization rate in the absence of Na⁺-MMT (i.e., $1.02 \times 10^{-4} - 4.80 \times 10^{-5} = 5.4 \times 10^{-5}$

$\text{mol dm}^{-3} \text{ s}^{-1}$). Fig. 2b shows that Na⁺-MMT has a significant effect on the reaction kinetics, especially during the early stage of polymerization. At [SDS] < CMC, the formation of particle nuclei via homogeneous nucleation is very slow, as shown by the X vs. t data for the polymerization in the absence of Na⁺-MMT in Fig. 2b. By contrast, the polymerization in the presence of Na⁺-MMT does not exhibit the characteristic of slow R_p . This implies that Na⁺-MMT platelets serve as additional reaction loci for the propagation reaction of radicals with monomer and they predominate in the early stage of polymerization.

In comparison with the run with 9 mM SDS and 1 wt.% Na⁺-MMT, the polymerization with 9 mM SDS and comparable ionic strength or conductivity (2000–2010 $\mu\text{S cm}^{-1}$, see the specific conductivity vs. [SDS] data in Fig. 1b) but in the absence of Na⁺-MMT was carried out to verify the proposed polymerization mechanisms. The increased conductivity of the polymerization system without Na⁺-MMT was achieved by the addition of NaCl. The values of R_p are 7.00×10^{-4} and $6.29 \times 10^{-4} \text{ mol dm}^{-3} \text{ s}^{-1}$ for the polymerizations with and without 1 wt.% Na⁺-MMT, respectively. However, the value of R_p for the run with 9 mM SDS and in the absence of both the Na⁺-MMT and additionally added NaCl is $5.98 \times 10^{-4} \text{ mol dm}^{-3} \text{ s}^{-1}$. Thus, the ionic strength effect alone cannot account for the much stronger increased R_p arising from the use of 1 wt.% Na⁺-MMT (see the $(R_p - R_{p,0})/R_{p,0}$ data for the run with [SDS] = 9 mM in Table 1). Furthermore, the featureless XRD spectrum of the PS/Na⁺-MMT (93.3/6.7 (w/w)) sample obtained from the polymerization with 9 mM SDS and 1 wt.% Na⁺-MMT suggests that the probability for the regular structure of Na⁺-MMT platelets to weaken or even disappear after the completion of the polymerization is quite high (Fig. 5), which is consistent with the literature [16]. It is noteworthy that, at this level of Na⁺-MMT, the XRD instrument should be capable of detecting the multiple-layered

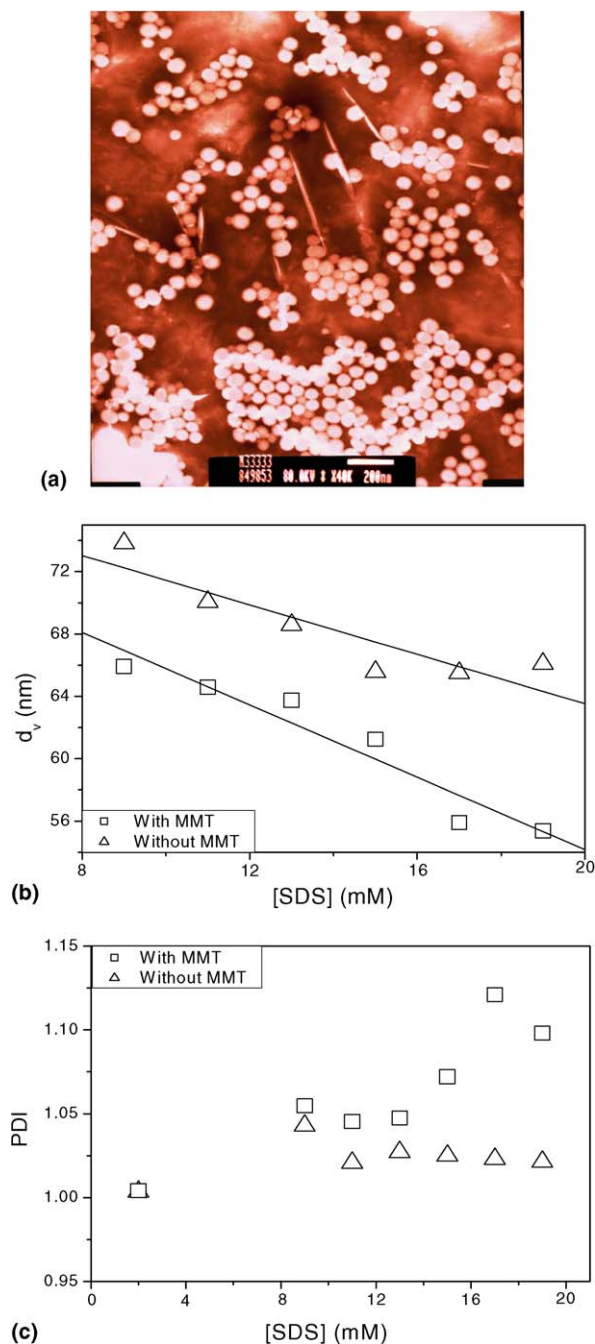


Fig. 4. (a) A representative TEM photograph for the Na^+ -MMT-containing polymerization with $[\text{SDS}] = 13 \text{ mM}$; (b) final latex particle diameter as a function of the bulk SDS concentration; (c) polydispersity index of the particle size distribution as a function of the bulk SDS concentration. Na^+ -MMT (wt.%) = (\square) 1, (\triangle) 0.

structure of Na^+ -MMT (if present) dispersed in the amorphous PS matrix. In addition, Table 1 shows that a significant increase in R_p was achieved when

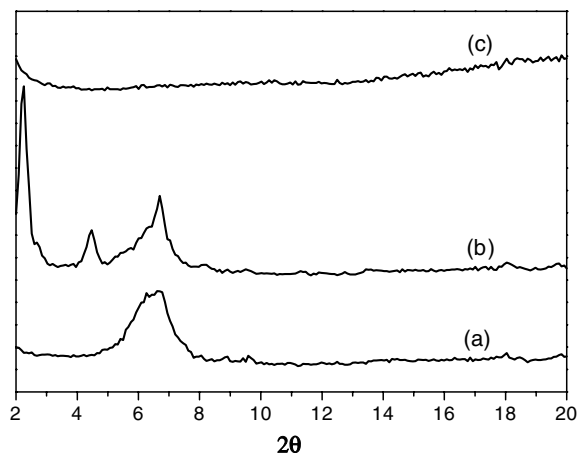


Fig. 5. X-ray powder diffraction spectra of (a) Na^+ -MMT dispersed in the aqueous solution of 2.66 mM NaHCO_3 , (b) Na^+ -MMT dispersed in the aqueous solution of 2.66 mM NaHCO_3 and 9 mM SDS , and (c) the PS/ Na^+ -MMT (93.3/6.7 (w/w)) sample obtained from the polymerization with 2.66 mM NaHCO_3 , 9 mM SDS and $1 \text{ wt.}\% \text{ Na}^+$ -MMT.

$1 \text{ wt.}\% \text{ Na}^+$ -MMT was added to the polymerization in the absence of micelles ($[\text{SDS}] = 2 \text{ mM}$). All these results provide supporting evidence for the contribution of Na^+ -MMT to the enhanced polymerization rate.

M_w increases with increasing $[\text{SDS}]$ for both the polymerizations with and without Na^+ -MMT (Fig. 6). This is attributed to the enhanced segregation of radicals inside the particles with increasing $[\text{SDS}]$ (i.e., N_p) ($N_p \sim [\text{SDS}]^{0.47}$, $r^2 = 0.9350$ for the runs without Na^+ -MMT). The segregation effect reduces the probability of bimolecular termination via the entry of a radical into the particle already containing one radical. Furthermore, at constant $[\text{SDS}]$, the M_w of the polymerization with Na^+ -MMT is larger than that of the counterpart without Na^+ -MMT. One possible explanation for this observation is the competitive absorption of radicals by Na^+ -MMT platelets that further depresses the bimolecular termination reaction in the latex particles. It should be noted that the difference in M_w between the polymerizations with and without Na^+ -MMT increases with decreasing $[\text{SDS}]$. This shows supporting evidence of the important role of Na^+ -MMT platelets for the polymerizations stabilized by relatively low levels of surfactant.

The zeta potential (ζ) of the latex particles and Na^+ -MMT platelets (if present) data are shown in Fig. 7. The absolute value of ζ increases with increasing $[\text{SDS}]$ for the polymerizations in the

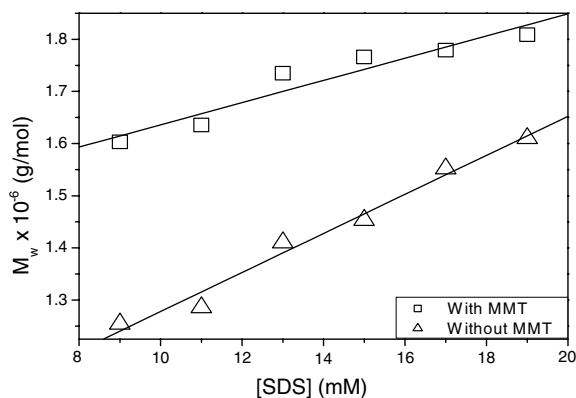


Fig. 6. Polymer molecular weight as a function of the bulk SDS concentration. Na⁺-MMT (wt.%) = (□) 1, (△) 0.

absence of Na⁺-MMT, whereas a reverse trend is observed for the polymerizations in the presence of Na⁺-MMT. Although the data are somewhat scattered for the polymerizations with Na⁺-MMT ($r^2 = 0.8057$, Fig. 8), the ζ data correlate reasonably well with the particle surface charge density, $[\text{SDS}]/(\pi d_p^2 N_p)$. For the purpose of demonstration only, the assumption that all the polymer chains form in the latex particles has been made to construct the ζ vs. $[\text{SDS}]/(\pi d_p^2 N_p)$ plot for the polymerizations with Na⁺-MMT. It is postulated that the scattered data reflect the influence of Na⁺-MMT on the electrophoretic properties. As expected, ζ increases with increasing particle surface charge density (Fig. 8).

In the presence of Na⁺-MMT, R_p during the constant reaction rate period can be expressed as

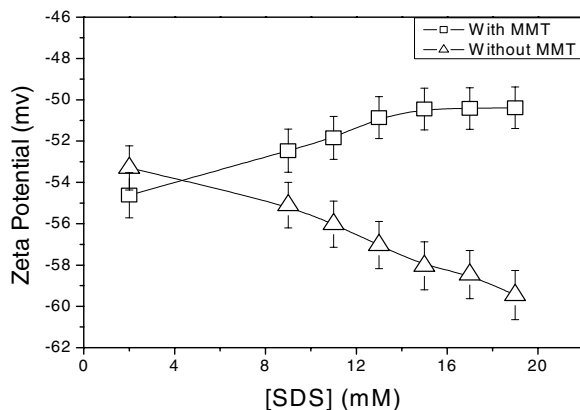


Fig. 7. Zeta potential of latex particles and Na⁺-MMT platelets (if present) as a function of the bulk SDS concentration. Na⁺-MMT (wt.%) = (□) 1, (△) 0.

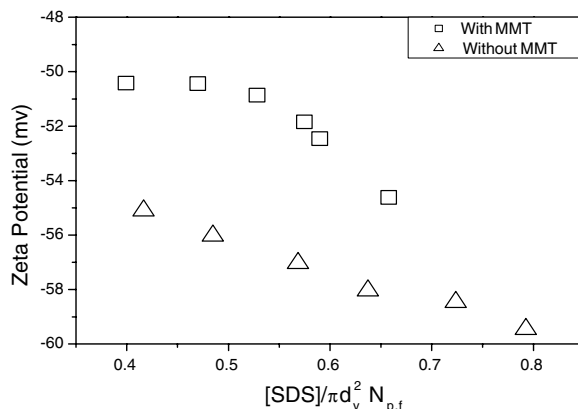


Fig. 8. Zeta potential of latex particles and Na⁺-MMT platelets (if present) as a function of the surface charge density. Na⁺-MMT (wt.%) = (□) 1, (△) 0.

$$R_p = R_{p,0} + R_{p,\text{MMT}} = k_{p,0}[\text{M}]_p(n_p N_{p,0}/N_A) + k_{p,\text{MMT}}[\text{M}]_{\text{MMT}}(n_{\text{MMT}} N_{\text{MMT}}/N_A) \quad (2)$$

$$N_{p,0} = [W_m X_f / (\pi / 6 d_p^3 \rho_p W_w)] \omega \quad (3)$$

$$N_{\text{MMT}} = N_{\text{MMT,t}} / n_{\text{agg,MMT}} \quad (4)$$

$$n_p = 1/2 \{ -\alpha'/m + [(\alpha'/m)^2 + 2\alpha'/m]^{1/2} \} \quad (5)$$

when $n_p \leq 0.5$

where the subscripts 0 and MMT represent the related kinetic parameters associated with the latex particles and Na⁺-MMT platelets, respectively. W_m is the total monomer weight, X_f the final fractional monomer conversion, ρ_p the polymer density, W_w the total water weight, ω the degree of contribution of the polymerization in latex particles ($0 \leq \omega \leq 1$). N_{MMT} is the number of Na⁺-MMT platelets per unit liter water, $N_{\text{MMT,t}}$ the total number of the smallest units of multiple-layered Na⁺-MMT platelets (each platelet with approximate dimensions of $100 \times 100 \times 1 \text{ nm}^3$ and total particle surface area of $2.04 \times 10^4 \text{ nm}^2$ [23]), and $n_{\text{agg,MMT}}$ the number of platelets per stack. The empirical Eq. (5) derived by Nomura [24] was used to calculate n_p . $\alpha' [= \rho_i v_p / (k_t N_p)]$ is the dimensionless group associated with the absorption of radicals by the latex particles, $m (= k_{\text{des}v_p} / k_t)$ is the dimensionless group associated with the desorption of radicals out of the particles, ρ_i is equal to $2fk_d[I]$, f is defined as the initiator efficiency factor in the polymerizations containing 1 wt.% Na⁺-MMT that takes into account the effect of the presence of 1 wt.% Na⁺-MMT on the absorption of free radicals by the latex particles, $k_d [= 6.06 \times 10^{16} \exp(-140,167/RT) \text{ s}^{-1}]$ [25] is the initiator decomposition rate constant, $[I]$

is the initiator concentration, v_p is the volume of a particle, k_t [$=8.2 \times 10^9 \exp(-14,510/RT) \text{ dm}^3 \text{ mol}^{-1} \text{ s}^{-1}$] [26] is the termination rate constant, and k_{des} [$=k'_{\text{des}}/(v_p)^{2/3}$] [27] is the desorption rate constant. In addition to the above parameters, the following parameters obtained from the literature or estimated in this work were used to carry out computer simulations: $k_{p,0} = k_{p,\text{MMT}} = 4.27 \times 10^7 \exp(-32,510/RT) \text{ dm}^3 \text{ mol}^{-1} \text{ s}^{-1}$ [28], $[M]_p = [M]_{\text{MMT}} = 5.2 \text{ M}$ [29], $[I] = 2.59 \text{ mM}$, $k'_{\text{des}} = (1.94 \pm 0.86) \times 10^{-11} \text{ cm}^2 \text{ s}^{-1}$ at 70°C based on the kinetic data obtained from the polymerizations in the absence of Na^+ -MMT in this study, and $N_{\text{MMT},t} = 4.42 \times 10^{17} \text{ dm}^{-3}$ estimated by dividing the total Na^+ -MMT platelet surface area ($7.5 \times 10^{20} \text{ nm}^2 \text{ g}^{-1} \times 12.02 \text{ g dm}^{-3}$) by $2.04 \times 10^4 \text{ nm}^2$, where the specific Na^+ -MMT platelet surface area ($7.5 \times 10^{20} \text{ nm}^2 \text{ g}^{-1}$) was taken from the literature [30,31].

Eqs. (2)–(5) were first used to qualitatively study the effect of the flux of free radicals toward the latex particles ($f = 0.1, 0.3$ or 0.5) on the polymerization mechanisms and kinetics in the presence of 1 wt.% Na^+ -MMT. Some representative contour plots of the $n_{\text{agg,MMT}}$ vs. ω data for the polymerizations with $[\text{SDS}] = 13 \text{ mM}$ and $n_{\text{MMT}} = 0.5$ are shown in Fig. 9a. At constant f , $n_{\text{agg,MMT}}$ increases with increasing ω and this trend becomes more pronounced when f increases from 0.1 to 0.5. This is simply due to the fact that the larger the contribution of polymerization in the latex particles (i.e., the larger value of ω or $N_{p,0}$) is, the slower the rate of polymerization in the Na^+ -MMT platelets (i.e., the larger value of $n_{\text{agg,MMT}}$ or the smaller value of N_{MMT}) is required to achieve the same total polymerization rate (R_p). It should be noted that the smaller the value of $n_{\text{agg,MMT}}$, the better the dispersion of Na^+ -MMT platelets in the reaction system. Na^+ -MMT becomes completely exfoliated when $n_{\text{agg,MMT}}$ approaches unity. It was reported that the pristine Na^+ -MMT existed in agglomerates of 1–10 μm in diameter, which comprised primary units of about 8–10 layered silicate platelets in each stack ($n_{\text{agg,MMT}} = 8$ –10) [32]. The Na^+ -MMT subject to intensive shear force and strong interactions between the surface active radicals and the highly swollen platelets should exist at least in the primary unit form and, therefore, have a $n_{\text{agg,MMT}}$ value smaller than 10. Similar results were also observed for the polymerizations with $[\text{SDS}] = 13 \text{ mM}$ and $n_{\text{MMT}} = 0.75$ and 1 (Fig. 9b and c). These preliminary simulation results also suggest that lower flux of free radicals toward the latex particles (i.e., smaller values of f)

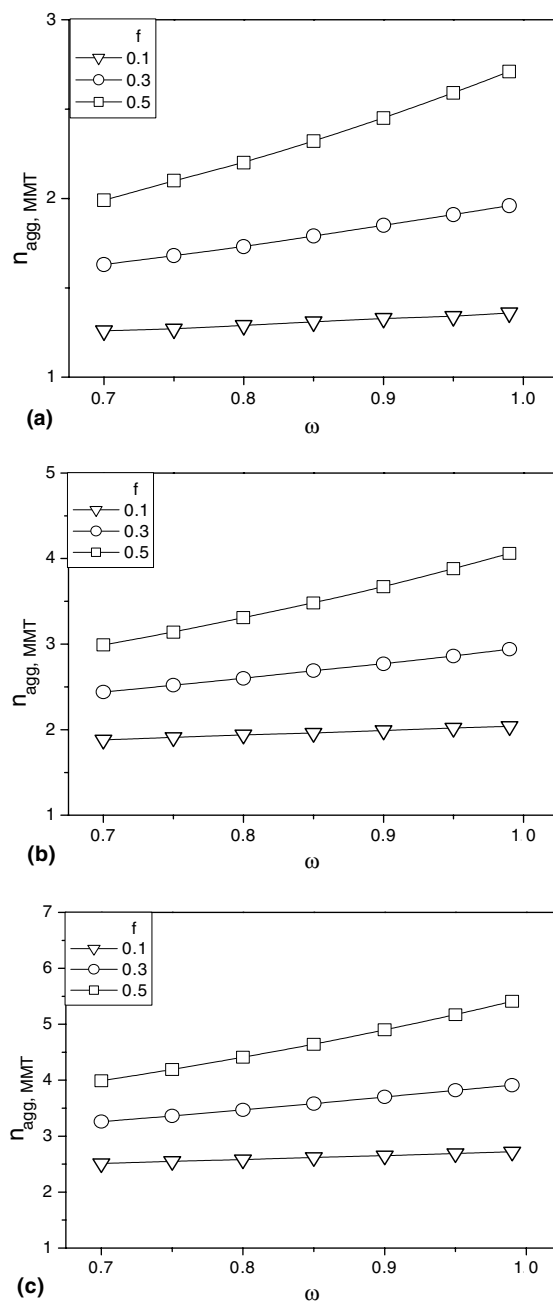
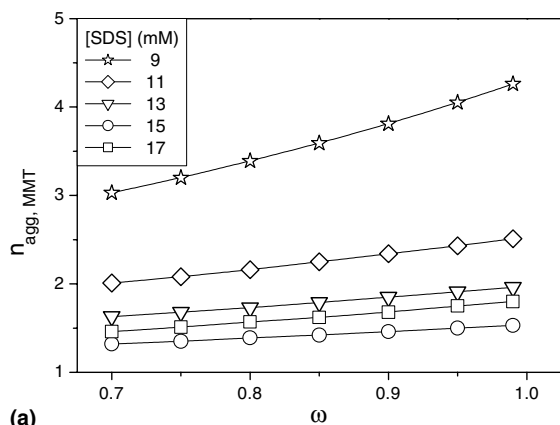


Fig. 9. Contour plots of the $n_{\text{agg,MMT}}$ vs. ω data for the polymerizations with 1 wt.% Na^+ -MMT, $[\text{SDS}] = 13 \text{ mM}$ and different values of f . (a) $n_{\text{MMT}} = 0.5$; (b) $n_{\text{MMT}} = 0.75$; (c) $n_{\text{MMT}} = 1.0$. (f) (□) 0.1, (○) 0.3, (▽) 0.5.

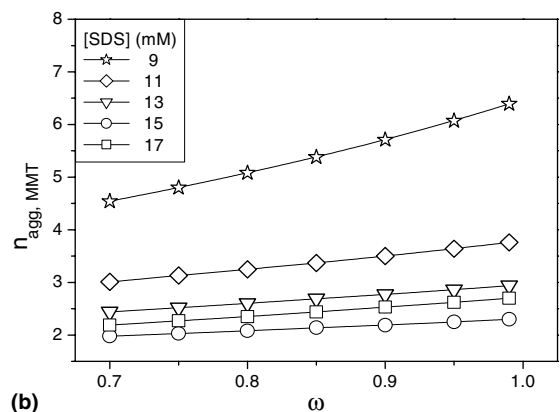
and less contribution of the polymerization in the latex particles (i.e., smaller values of ω (or $N_{p,0}$) and n_{MMT}) promote the intercalation or even exfoliation of Na^+ -MMT platelets in the aqueous phase.

This model was then used to study the effect of $[\text{SDS}]$ (9, 11, 13, 15 and 17 mM) on the polymeri-

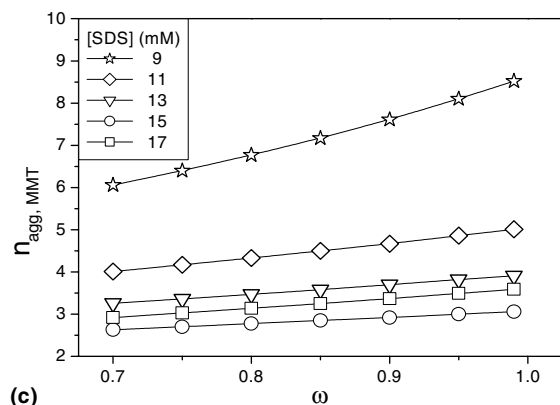
zation mechanisms and kinetics in the presence of 1 wt.% Na⁺-MMT. The parameter f was kept constant at 0.3 in this series of computer simulations. Fig. 10 shows some representative contour plots of the $n_{\text{agg,MMT}}$ vs. ω data for the polymerizations



(a)



(b)



(c)

Fig. 10. Contour plots of the $n_{\text{agg,MMT}}$ vs. ω data for the polymerizations with 1 wt.% Na⁺-MMT, $f=0.3$ and various bulk concentrations of SDS. (a) $n_{\text{MMT}} = 0.5$; (b) $n_{\text{MMT}} = 0.75$; (c) $n_{\text{MMT}} = 1.0$. [SDS] (mM): (\star) 9, (\diamond) 11, (∇) 13, (\circ) 15, (\square) 17.

with different values of [SDS] and n_{MMT} . At $n_{\text{MMT}} = 0.75$ and constant [SDS], $n_{\text{agg,MMT}}$ increases with increasing ω and this trend becomes more pronounced when [SDS] decreases from 17 to 9 mM (Fig. 10b). This is because the larger the contribution of the polymerization in the latex particles (i.e., the larger value of ω or $N_{p,0}$) is, the slower the rate of polymerization in the Na⁺-MMT platelets (i.e., the larger value of $n_{\text{agg,MMT}}$ or the smaller value of N_{MMT}) is required to achieve the same total polymerization rate (R_p). At constant ω , $n_{\text{agg,MMT}}$ decreases with increasing [SDS], but this effect becomes smaller when [SDS] increases from 9 to 17 mM. These simulation results again indicate that the effect of Na⁺-MMT on the polymerization kinetics becomes more important for the polymerizations stabilized by lower levels of SDS. In addition, the calculated results suggest that the probability of intercalating or even exfoliating the Na⁺-MMT platelets increases with increasing [SDS]. Thus, the results in Fig. 10b are reasonable for the Na⁺-MMT-containing polymerizations with [SDS] = 9–17 mM. The contour plots at $n_{\text{MMT}} = 0.5$ (Fig. 10a) and at $n_{\text{MMT}} = 1.0$ (Fig. 10c) exhibit very similar characteristic to the contour plot at $n_{\text{MMT}} = 0.5$ (Fig. 10b), but $n_{\text{agg,MMT}}$ shifts toward a region with larger values when n_{MMT} increases from 0.5 to 1.0 (Fig. 10).

It is noteworthy that the $n_{\text{agg,MMT}}$ value may decrease and, consequently, N_{MMT} may increase with the progress of polymerization. In addition, the location (the interlayer between two adjacent Na⁺-MMT platelets or the surfaces of Na⁺-MMT agglomerates) of the polymerization associated with Na⁺-MMT and the morphology of Na⁺-MMT platelets may also change significantly during polymerization. All these factors will make the polymerization mechanisms and kinetics even more complicated. It should be noted that Eqs. (2)–(5) only represent a preliminary model in an attempt to simulate the ST emulsion polymerization in the presence of 1 wt.% Na⁺-MMT. In order to gain an insight into the ST emulsion polymerization in the presence of Na⁺-MMT, more independent experiments are required to determine some of the parameters.

4. Conclusions

The influence of the pristine Na⁺-MMT platelets (1 wt.%) on the ST emulsion polymerizations with

different concentrations of SDS ($[SDS] = 2\text{--}19\text{ mM}$) was investigated. For comparison, the corresponding polymerizations in the absence of Na^+ -MMT were also carried out. The experimental data showed that, at constant $[SDS]$, the polymerization rate is faster for the run with Na^+ -MMT compared to the counterpart without Na^+ -MMT. This was attributed to the higher concentration of micelles (if present) for particle nucleation and the Na^+ -MMT platelets served as reaction loci. Micelle nucleation predominates in the ST emulsion polymerizations with $[SDS] \geq 13\text{ mM}$. On the other hand, the contribution of the polymerization associated with Na^+ -MMT platelets increases significantly when $[SDS]$ decreases from 13 to 9 mM. When $[SDS]$ is below the CMC, homogeneous nucleation controls the polymerization kinetics. Moreover, the contribution of Na^+ -MMT platelets to the polymerization kinetics is even comparable to the run without Na^+ -MMT. The differences in the resultant polymer particle size, polymer molecular weight and zeta potential between the polymerizations in the presence and absence of 1 wt.% Na^+ -MMT were investigated. A preliminary model was developed to qualitatively study the effect of the presence of 1 wt.% Na^+ -MMT on the polymerization mechanisms and kinetics.

References

- [1] Harkins WD. *J Chem Phys* 1945;13:381.
- [2] Harkins WD. *J Chem Phys* 1946;14:47.
- [3] Harkins WD. *J Am Chem Soc* 1947;69:1428.
- [4] Smith WV. *J Am Chem Soc* 1948;70:3695.
- [5] Smith WV, Ewart RH. *J Chem Phys* 1948;16:592.
- [6] Smith WV. *J Am Chem Soc* 1949;71:4077.
- [7] Priest WJ. *J Phys Chem* 1952;56:1977.
- [8] Roe CP. *Ind Eng Chem* 1968;60:20.
- [9] Fitch RM, Tsai CH. In: Fitch RM, editor. *Polymer colloids*. New York: Plenum Press; 1971. p. 73.
- [10] Fitch RM, Tsai CH. In: Fitch RM, editor. *Polymer colloids*. New York: Plenum Press; 1971. p. 103.
- [11] Fitch RM. *Br Polym J* 1973;5:467.
- [12] Choi YS, Choi MH, Wang KH, Kim SO, Kim YK, Chung IJ. *Macromolecules* 2001;34:8978.
- [13] Choi YS, Wang KH, Xu M, Chung IJ. *Chem Mater* 2002;14:2936.
- [14] Kim TH, Jang LW, Lee DC, Choi HJ, Jhon MS. *Macromol Rapid Commun* 2002;23:191.
- [15] Kim BH, Jung JH, Hong SH, Joo J, Epstein AJ, Mizoguchi K, et al. *Macromolecules* 2002;35:1419.
- [16] Kim YK, Choi YS, Wang KH, Chung IJ. *Chem Mater* 2002;14:4990.
- [17] Goddard ED, Benson GC. *Can J Chem* 1957;35:986.
- [18] Mukerjee P, Mysels KJ, Dulin CI. *J Phys Chem* 1958;62:1390.
- [19] Chang HC, Lin YY, Chern CS, Lin SY. *Langmuir* 1998;14:6632.
- [20] Hayase K, Hayano S. *Bull Chem Soc Jpn* 1977;50:83.
- [21] Jain AK, Singh RPB. *J Colloid Interf Sci* 1981;81:536.
- [22] Hunter RJ. *Foundations of colloid science*, vol. 1. New York: Oxford; 1989. p. 598.
- [23] Usuki A, Hasegawa N, Kadoura H, Okamoto T. *Nano Letters* 2001;1:271.
- [24] Nomura M. In: Piirma I, editor. *Emulsion polymerization*. New York: Academic; 1982. p. 191.
- [25] Kolthoff IM, Miller IK. *J Am Chem Soc* 1951;73:3055.
- [26] Matheson MS, Auer EE, Bevilacqua EB, Hart EJ. *J Am Chem Soc* 1951;73:1700.
- [27] Lee HC, Poehlein GW. *Polym Process Eng* 1987;5:37.
- [28] Gilbert RG. *Pure Appl Chem* 1996;68:1491.
- [29] Bartholome E, Gerrens H, Herbeck R, Weitz HM. *Z Elektrochem* 1956;60:334.
- [30] Lefebvre Y, Lacelle S, Jolicoeur C. *J Mater Res* 1992;7:1888.
- [31] Celis R, Cornejo J, Hermosin MC. *Clay Miner* 1996;31:355.
- [32] Akelah A, Moer A. *J Appl Polym Sci: Appl Polym Symp* 1994;55:153.